THE JOURNAL OF PHYSICAL CHEMISTRY B

Article

pubs.acs.org/JPCB

Influence of Solvent Polarity on Preferential Solvation of Molecular Recognition Probes in Solvent Mixtures

Valeria Amenta,[†] Joanne L. Cook,[†] Christopher A. Hunter,*[,†] Caroline M. R. Low,[‡] and Jeremy G. Vinter[§]

[†]Department of Chemistry, University of Sheffield, Sheffield, S3 7HF United Kingdom

[‡]Drug Discovery Facility, Imperial College, Rm 512 Biochemistry, London, SW7 2AY United Kingdom

[§]Cresset Biomolecular Discovery, BioPark Hertfordshire, Broadwater Road, Welwyn Garden City, AL7 3A United Kingdom

Supporting Information

ABSTRACT: The association constants for formation of 1:1 complexes between a H-bond acceptor, tri-*n*-butylphosphine oxide, and a H-bond donor, 4-phenylazophenol, have been measured in a range of different solvent mixtures. Binary mixtures of *n*-octane and a more polar solvent (ether, ester, ketone, nitrile, sulfoxide, tertiary amide, and halogenated and aromatic solvents) have been investigated. Similar behavior was observed in all cases. When the concentration of the more polar solvent is low, the association constant is identical to that observed in pure *n*-octane. Once a threshold concentration of the more polar solvent in reached, the logarithm of the association constant decreases in direct proportion to the logarithm of the concentration of the more polar solvent. This indicates that one of the two solutes is preferentially solvated by the more polar solvent, and it is competition with this solvation equilibrium that determines the observed association constant. The concentration of the more polar solvent at which the onset of preferential solvation takes place depends on solvent polarity: 700 mM for toluene, 60 mM for 1,1,2,2-tetrachloroethane, 20 mM for the ether, ester, ketone, and nitrile, 0.2 mM for the tertiary amide, and 0.1 mM for the sulfoxide solvents. The results can be explained by a simple model that considers only pairwise interactions between specific sites on the surfaces of the solutes and solvents, which implies that the bulk properties of the solvent have little impact on solvation thermodynamics.

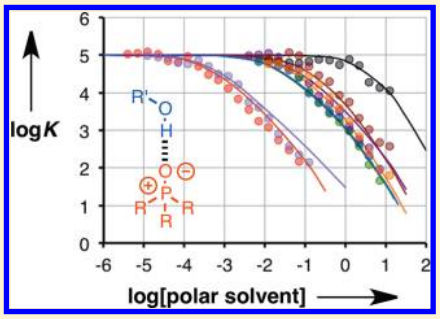

The choice of solvent has a profound influence on solubility, the spectroscopic properties of solutes, the affinity and selectivity of intermolecular interactions, the rate and mechanism of chemical reactions, as well as processes like crystallization. Many theoretical models have been developed to account for solvation phenomena: continuum models where the solvent is considered as a continuous and structureless medium that surrounds the solutes; supramolecular models that consider the solvent molecules around a solute in the same way as the solute itself; and semicontinuum models that consider the solute molecule along with the first solvation shell surrounded by a continuum solvent.[1−6] However, it is still difficult to make reliable quantitative predictions of solvent effects on chemical processes, and the description of processes in solvent mixtures is even more complicated, due to the occurrence of preferential solvation. Many techniques have been used to investigate preferential solvation experimentally: UV−vis absorption,[7−10] fluorescence,[11,12] NMR,[13−18] IR absorption,[19−22] calorimetry,[23−25] circular dichroism,[26] and mass spectrometry.[27] Most of these techniques involve the use of a molecular probe, which has a property that is sensitive to the solvent environment.[28] If no preferential solvation occurs, the property measured is a linear function of the solvent composition, and any deviation from linearity is indicative of preferential solvation. However, a more quantitative interpretation is difficult, because these experiments generally report on changes in the composition of the entire solvation shell of the solute. Preferential solvation leads to different compositions of the solvation shell at different parts of the molecular surface in a way that depends on the relative strengths of the solvent−solvent and solute−solvent interactions at different sites. This makes it difficult to deconvolute the various contributions that are solvent, solute, and site dependent. Computer simulation can be used to obtain some insight into the molecular details of complex solvation shells.[29]

We recently introduced the use of molecular recognition-based probes to study the molecular details of solvation thermodynamics.[30] Such probes are made by the combination of two solutes, a strong hydrogen bond donor (D) and a strong hydrogen bond acceptor (A). The strength of the solute−solute binding interaction in a binary solvent mixture is dependent on solvation equilibria that involve just one site on the surface of each solute molecule (Figure 1). The use of these molecular recognition-based probes therefore allows one to dissect and quantify the different contributions made by specific solvation equilibria to the stability of a complex.[31] We have shown that the properties of these systems can be understood based on pairwise interactions at the most polar sites on the molecular

Received: October 19, 2012
Revised: November 15, 2012
Published: November 28, 2012

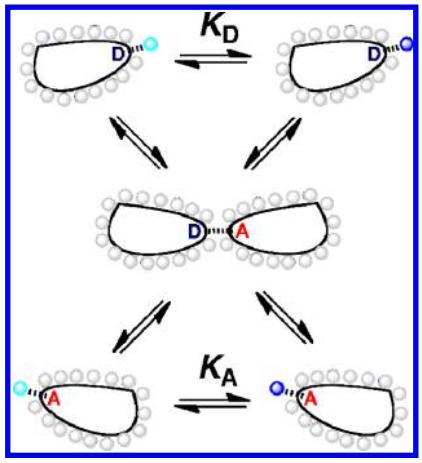

Figure 1. Molecular recognition probes of solvation allow characterization of interactions at individual binding sites on the solute surface. In a mixture of two solvents S1 and S2 (dark blue and light blue), the behavior of the system is determined by the thermodynamic properties of the five different species illustrated. The binding constant between A and D depends on the solvation of D by S1 and S2 (K_D) and the solvation of A by S1 and S2 (K_A). Selective solvation at any of the other sites on the solute surfaces (gray) has little impact on the equilibria.

surfaces of both solvent and solute. The bulk properties of the solvent do not appear to play a significant role, and the solvation equilibria at the other sites on the solute surfaces have little impact on the stability of the D•A complex.

Specifically, the association constant (K) for formation of a H-bonded complex, D•A, in mixtures of alkanes (S1) and ethers (S2) was found to obey eq 1 for a wide range of solvent compositions.[31]

$$K = \frac{K_{S1}}{1 + K_D[S2]} \quad (1)$$

where K_{S1} is the D•A association constant in S1, K_D is the D•S2 association constant in S1.

At low concentrations of the more polar solvent (ether, S2), the association constant is independent of the concentration of S2, because there is insufficient S2 to compete with S1 for solvation of the solutes. However when the concentration of S2 is increased, a threshold is reached after which preferential solvation of the polar solutes by the polar solvent becomes significant. Figure 2 illustrates the effect on the observed association constant. For high concentrations of S2, the log K shows a linear dependence on log[S2], and the log K profile in Figure 2 has a slope of approximately −1. The onset of selective solvation is indicated by the black dot in Figure 2. The location of this point is the intercept of the horizontal and vertical dashed lines, which are defined by the association constant for the D•A complex in solvent S1 (K_{S1}) and the association constant for the formation of the D•S2 complex in solvent S1 (K_D). In the case of ether-alkane mixtures, solvation of the H-bond acceptor, A, is similar in S1 and S2, so the second solvation equilibrium shown in Figure 1 (K_A) has little effect on the observed association constant.

Qualitatively similar behavior was observed for four different molecular recognition probes in alkane-ether mixtures.[32] However, the onset of preferential solvation depends on the H-bond donor strength of D. As implied by eq 1, when D is a stronger H-bond donor, preferential solvation occurs at lower

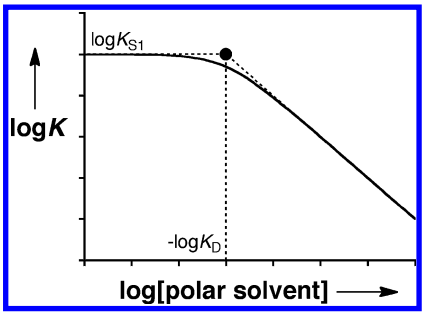

Figure 2. Solvent dependence of the association constant for formation of the D•A complex (K) in a mixture of a nonpolar solvent, S1, and a polar solvent, S2. The horizontal dashed line is related to the association constant for formation of the D•A complex in pure S1 (K_{S1}), and the vertical dashed line is related to the association constant for formation of the D•S2 complex in S1 (K_D).

concentrations of the more polar solvent, S2. These results suggest that it should be possible to make quantitative predictions of the solvation properties of solvent mixtures based on the H-bond donor/acceptor properties of the solvent and solutes and their concentrations. Here in an attempt to generalize this model, we report the properties of a molecular recognition probe in a wide range of different solvent mixtures.

RESULTS AND DISCUSSION

4-Phenylazophenol (D) is a very strong H-bond donor, and tri-*n*-butylphosphine oxide (**A**) is a very strong H-bond acceptor, so it is possible to measure association constants for formation of the D•A H-bond in relatively polar solvent mixtures (Figure 3). There is a characteristic change in the UV/vis absorption

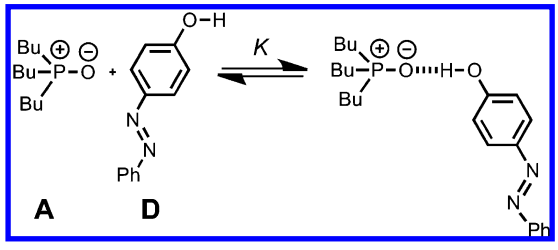

Figure 3. 1:1 complex formed between tri-*n*-butylphosphine oxide (A) and 4-phenylazophenol (D).

maximum of 4-phenylazophenol on formation of the H-bond, and this provides a convenient spectroscopic handle for determination of association constants using UV/vis titrations. A UV/vis plate reader was used to carry out automated titrations on this complex in eight binary solvent mixtures composed of *n*-octane (S1) and a more polar solvent (S2). In this paper, we describe the properties of solvents that contain ether, ester, ketone, nitrile, tertiary amide and sulfoxide functional groups. These represent examples of the most widely used classes of aprotic organic solvent, but we have used long chain versions of the common solvents, e.g., di-*n*-butyl sulfoxide in place of dimethyl sulfoxide, because this improves the miscibility with *n*-octane and minimizes losses due to evaporation. We also include examples of chlorinated and aromatic solvents, 1,1,2,2-tetrachloroethane and toluene. Protic solvents undergo significant self-association, which complicates the solvation properties, and these solvents will form the subject of separate study.

dx.doi.org/10.1021/jp310379h | J. Phys. Chem. B 2012, 116, 14433−14440

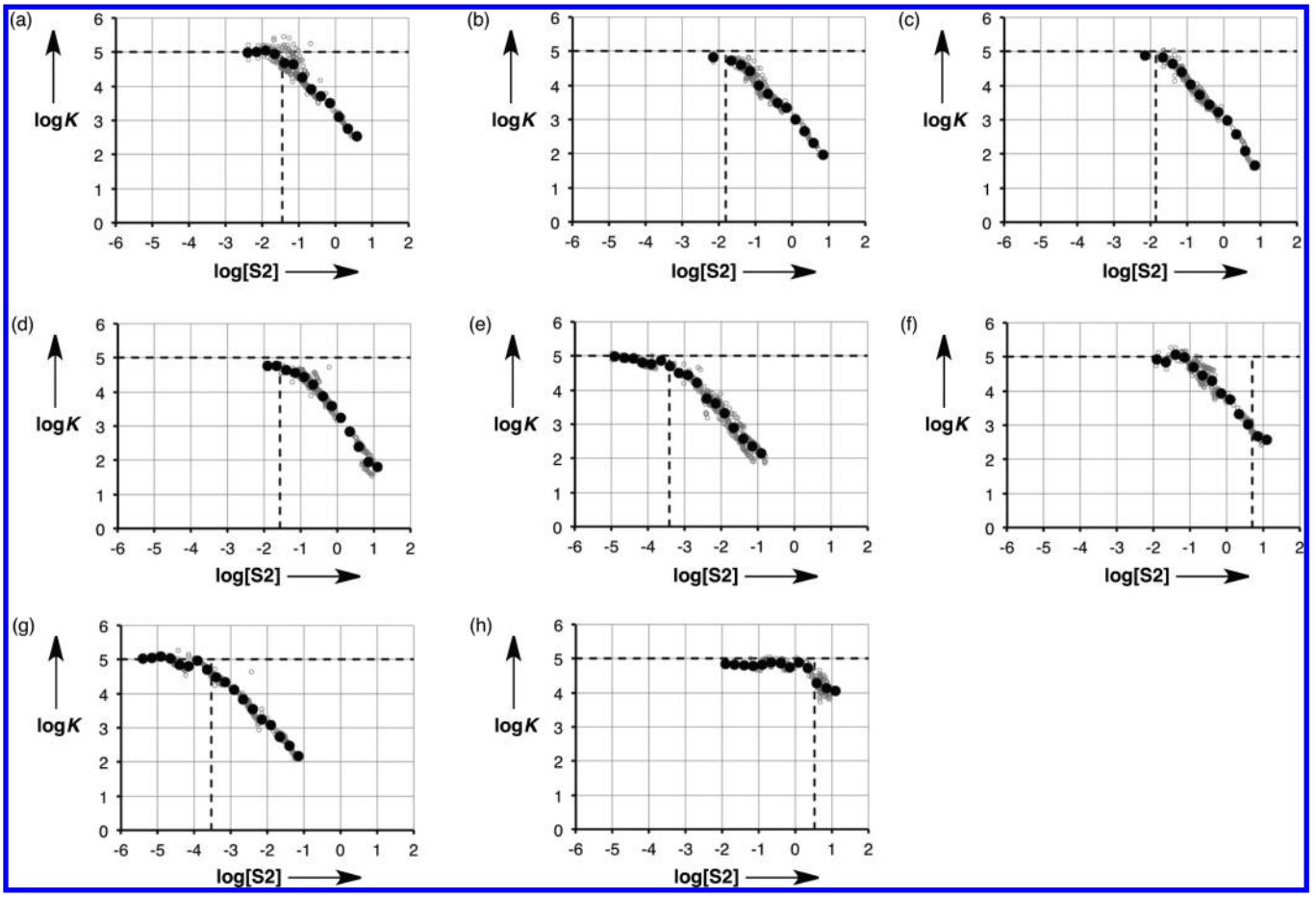

Figure 4. Association constant for formation of the D•A complex (K) plotted as a function of the concentration of S2 in mixtures of *n*-octane and a more polar solvent (S2). S2 is (a) di-*n*-octyl ether, (b) ethyl heptanoate, (c) 2-heptanone, (d) *n*-butyl cyanide, (e) *N*,*N*-diethyl acetamide, (f) 1,1,2,2-tetrachloroethane, (g) di-*n*-butyl sulfoxide, and (h) toluene. Open gray circles represent data from individual titrations, and filled black circles represent an average of the experimental data over a window of 0.25 units on the log *K* and log[S2] scale. The horizontal dashed lines are the value of log *K* measured in S1, and the vertical dashed lines are drawn at log[S2] = −log K_D.

The titration data fit well to a 1:1 binding isotherm in all cases, provided a linear correction term was included to account for the absorbance of A at high guest concentrations. The phenolate anion of D has an absorption maximum at 450 nm, and this was not detected in any of the experiments, so there is negligible proton transfer between A and D in the complex.[32] The stability of the D•A complex (log *K*) is plotted as a function of the concentration of S2 in the solvent mixture in Figure 4. The behavior is qualitatively similar in all of the solvent mixtures. At low concentrations of S2, the stability of the D•A complex is identical to that in pure *n*-octane. Once the concentration of the polar solvent is sufficient to compete effectively with the alkane for solvation of the solutes, log *K* decreases as a linear function of log[S2]. In this regime, the gradient is approximately −1 for all of the solvent mixtures. The threshold solvent concentration, which signifies the onset of preferential solvation by S2, is around 700 mM for toluene, 60 mM for the chlorinated solvent, 20 mM for the ether, ester, ketone, and nitrile solvents, 0.2 mM for the tertiary amide, and 0.1 mM for the sulfoxide.

It is possible to study the interaction of the polar solvents with the solutes independently by carrying out titrations in *n*-octane. The association constant for solvation of D by S2 (K_D) can be measured directly by titrating S2 into an *n*-octane solution of D and monitoring the change in the UV/vis absorption spectrum. No significant interaction was observed for 1,1,2,2-tetrachloroethane or toluene, but the results for the other solvents are shown in Figure 5. In *n*-octane, D has an absorption maximum at 339 nm, and this moves to 346 nm in di-*n*-octyl ether, 348 nm in ethyl heptanoate, 347 nm in 2-heptanone, 348 nm in *n*-butyl cyanide, 353 nm in *N*,*N*-diethylacetamide, and 351 nm in di-*n*-butyl sulfoxide. In some cases, there is no well-defined isosbestic point, which indicates that there are more processes than formation of a simple D•S2 complex. The titration data were therefore fit to a 1:1 binding isotherm allowing for second weaker binding event with an association constant fixed at 0.1 M^{-1} (effectively a linear correction for high S2 concentrations). This binding isotherm fit the experimental data well in all cases, and the results are reported in Table 1.

The values of K_D for the tertiary amide and sulfoxide solvents are 2 orders of magnitude higher than the values measured for the ether, ester, ketone and nitrile solvents. This is consistent with the solvent H-bond acceptor parameters (β_S) listed in Table 1. Amides and sulfoxides are much better H-bond acceptors and therefore interact more strongly with good H-bond donors like D. The two solvents for which binding could not be measured, toluene and 1,1,2,2-tetrachloroethane, are exceptionally weak H-bond acceptors. The values of K_D in Table 1 can be used to account for the onset of selective

dx.doi.org/10.1021/jp310379h | J. Phys. Chem. B 2012, 116, 14433−14440

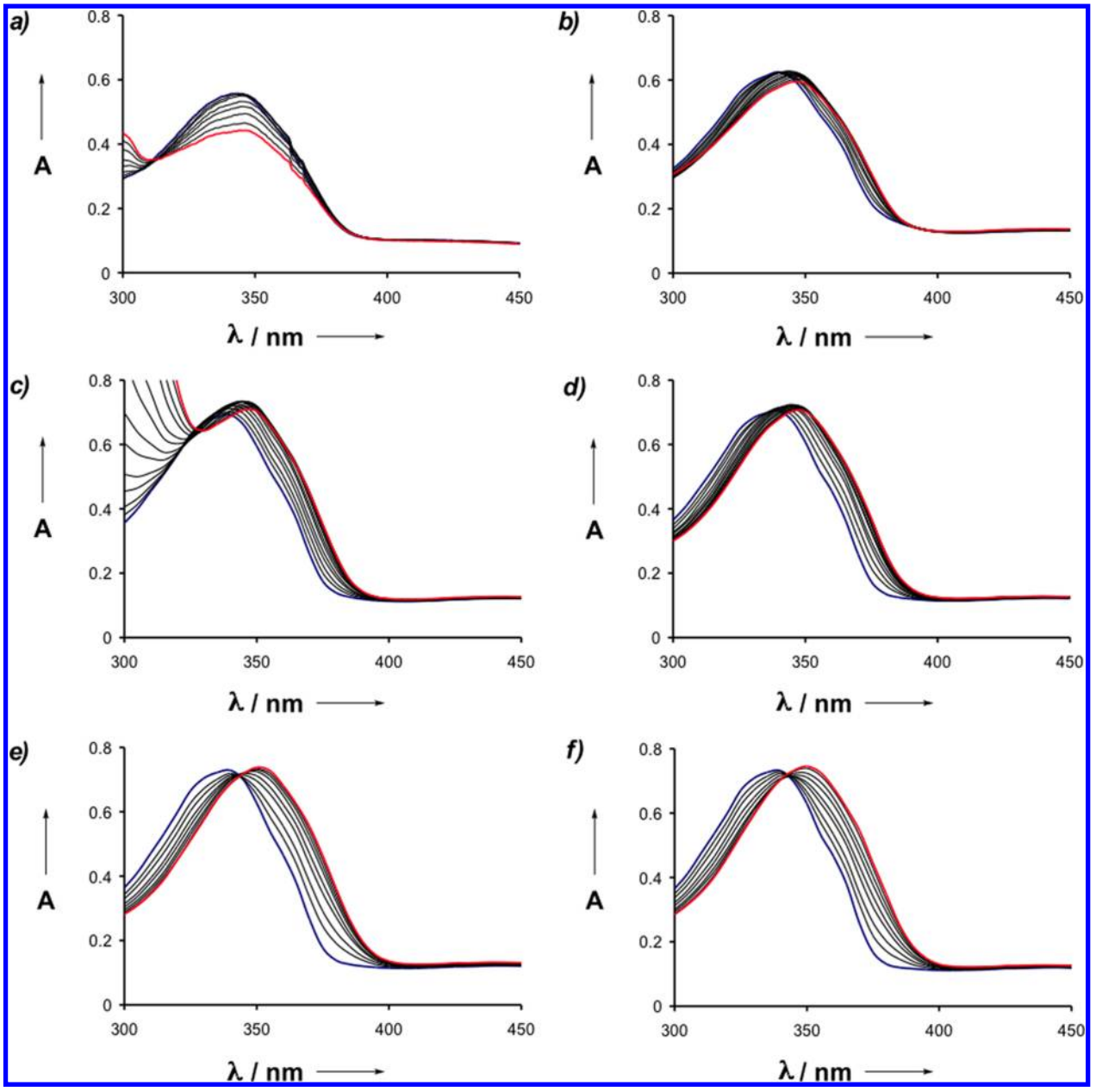

Figure 5. UV−vis absorption spectra for titration of (a) di-*n*-octyl ether, (b) ethyl heptanoate, (c) 2-heptanone, (d) *n*-butyl cyanide, (e) *N*,*N*-diethyl acetamide, and (f) di-*n*-butyl sulfoxide into D in *n*-octane. The spectra of unbound D are shown in blue and the D•S2 complex in red.

Table 1. Association Constants for Formation of 1:1 Complexes between S2 and D (K_D/M^{-1}) and between S2 and A (K_A/M^{-1}) in *n*-Octane at 298 K[a]

			experimental		calculated[a]	
S2	α_{S2}	β_{S2}	K_D[b]	K_A[c]	K_D[d]	K_A[e]
di-*n*-octylether	0.9	5.3	28 ± 8		45	0.1
ethyl heptanoate	1.5	5.3	65 ± 10		45	0.3
2-heptanone	1.5	5. 8	72 ± 20		87	0.3
N-butyl cyanide	1.7	5.2	37 ± 4		39	0.4
N,*N*-diethylacetamide	1.5	8.5	2600 ± 400		3800	0.3
1,1,2,2-tetrachloethane	2.0	1.3		15 ± 2	0.2	4
di-*n*-butyl sulfoxide	2.2	8.7	3400 ± 500		4000	9
toluene	1.1[c]	1.6			0.3	0.1

[a]Experimental results are the average of at least three titrations and the errors are quoted at the 95% confidence limit. [b]Measured by UV/vis titrations. [c]Measured by ^{31}P NMR titrations. [d]Calculated using the solvent H-bond parameter β_{S2} in eq 2.[33,34] [e]Calculated using the solvent H-bond parameter α_{S2} in eq 3.[33−35]

dx.doi.org/10.1021/jp310379h | J. Phys. Chem. B 2012, 116, 14433−14440

solvation observed in Figure 4. D is 50% solvated by S2, when $K_D[S2] = 1$ or $[S2] = 1/K_D$. This point is marked by a vertical dashed line in each of the panels in Figure 4 ($\log[S2] = -\log K_D$). These lines coincide with the point at which the gradient of the log$K$ profile changes from zero to −1, i.e., the point at which solvation of D by S2 starts to compete with solvation by S1. The slope of −1 indicates that the number of S2 molecules that compete with **A** for binding to D is one, and the experiment therefore provides a direct probe of the solvation of a single site on the surface of D.

It is possible to estimate the value of K_D using eq 2 and the relevant H-bond parameters.

$$-RT \ln K_D = -(\alpha_D - \alpha_{S1})(\beta_{S2} - \beta_{S1}) + 6 \text{ kJ mol}^{-1} \quad (2)$$

where α_D is the H-bond donor parameter of the solute D, β_{S2} is the H-bond acceptor parameter of S2, and α_{S1} and β_{S1} are corresponding H-bond parameters of *n*-octane. The values of β_{S2} are given in Table 1, $\alpha_D = 4.3$, $\alpha_S = 1.0$, and $\beta_S = 0.6$.[36]

The values of K_D calculated using eq 2 are in good agreement with the experimental values in all cases. For toluene and 1,1,2,2-tetrachloroethane, the K_D values are too low to be measured experimentally, so the calculated values were used to construct the vertical dashed lines for these two solvents in Figure 4. For toluene, this line coincides with the point at which the gradient of the log K profile changes from 0 to −1 (Figure 4h). However, this is not the case for 1,1,2,2-tetrachloroethane (Figure 4f). The calculated value of K_D predicts the onset of selective solvation of D at a concentration of S2 of 500 mM ($1/K_D$), but the change in the gradient of the log K profile takes place at a concentration of S2 that is an order of magnitude lower. This suggests that there is a different solvation process that dominates in 1,1,2,2-tetrachloroethane. Examination of the H-bond parameters in Table 1 reveals that 1,1,2,2-tetrachloroethane is the worst H-bond acceptor of the solvents used in this study, but it is a relatively good H-bond donor. The association constant for solvation of A by S2 (K_A) can be estimated using eq 3 and the relevant H-bond parameters.

$$-RT \ln K_A = -(\alpha_{S2} - \alpha_{S1})(\beta_A - \beta_{S1}) + 6 \text{ kJ mol}^{-1} \quad (3)$$

where β_A is the H-bond acceptor parameter of the solute A, α_{S2} is the H-bond donor parameter of S2, and α_{S1} and β_{S1} are corresponding H-bond parameters of *n*-octane. The values of α_{S2} are given in Table 1, $\beta_A = 10.2$, $\alpha_S = 1.0$, and $\beta_S = 0.6$.[36]

The calculated value of K_A for 1,1,2,2-tetrachloroethane in Table 1 is an order of magnitude higher than the calculated value of K_D suggesting that it is indeed solvation of A that dominates in this solvent. The value of K_A is large enough to measure experimentally, and this was achieved using ^{31}P NMR spectroscopy. The change in the ^{31}P NMR chemical shift of A was monitored titrating S2 into an *n*-octane solution of A. The titration data fit well to a 1:1 binding isotherm (Figure 6), and the result in Table 1 confirms that 1,1,2,2-tetrachloroethane preferentially solvates A rather than D. A is 50% solvated by S2, when $K_A[S2] = 1$, or $[S2] = 1/K_A$. This concentration of S2 corresponds to the point at which the gradient of the log K profile changes from 0 to −1 in Figure 4f ($\log[S2] \approx -1$).

The 1,1,2,2-tetrachloroethane results highlight the importance of solvation of the H-bond acceptor as well as solvation of the donor and suggest that eq 1 can be generalized as eq 4 for solvents where there are no strong solvent−solvent interactions.

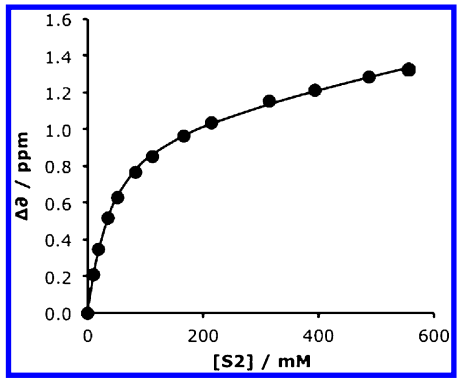

Figure 6. ^{31}P NMR titration of 1,1,2,2-tetrachloroethane into A in *n*-octane at 298 K. The line is the best fit to a 1:1 binding isotherm allowing for a second weaker nonspecific binding interaction.

$$K = \frac{K_{S1}}{(1 + K_D[S2])(1 + K_A[S2])} \quad (4)$$

When $K_A[S2]$ is significantly less than 1, eq 4 reduces to eq 1. Equation 4 can be used with the values of K_A and K_D in Table 1 to calculate log K profiles for each of the solvent mixtures. The black lines in Figure 7 show the results, which agree well with the experimental data. The dotted lines in Figure 7 were calculated using eq 1, which ignores solvation of **A** by S2. The deviation between the two sets of calculated values is largest for the 1,1,2,2-tetrachloroethane experiment (Figure 7f), where solvation of A by S2 is more important than solvation of D. However, the use of both the K_A and K_D terms in eq 4 significantly improves the agreement of the calculated lines with the experimental profiles in all cases. In most solvent mixtures, the interaction of S2 with A is through relatively weak C−H···O H-bonds, but these interactions become important at high S2 concentrations accounting for the experimentally observed curvature in the log K profiles at high S2 concentrations.

In general, the solvation equilibria that are considered should also include solvent−solvent interactions, but for solvent mixtures where either or both of α_S and β_S are small, the solvent−solvent term is negligible compared with the solvent−solute interactions, and eq 4 provides a good description of the properties of the system. For strongly self-associated solvents, like alcohols, the solvation properties of solvent mixtures will be more complicated. The approach described here focuses on solvation of a single functional group, but the composition of the solvation shell at any point on the surface of a molecule will vary in a way that depends on the polarity of the surface functionality: for the solvent systems described here, stronger preferential solvation will be observed at more polar sites.[32]

■ CONCLUSIONS

A molecular recognition approach has been used to study the solvation properties of mixtures of *n*-octane and a range of organic solvents that contain different polar functional groups. When the concentration of the more polar solvent S2 is low, the A•D complex has the same stability as in pure *n*-octane. When the concentration of S2 increases above a certain threshold, the logarithm of the association constant decreases as a linear function of the logarithm of the concentration of S2. This is due to preferential solvation of A when S2 is 1,1,2,2-tetrachloroethane and due to preferential solvation of D for all of the other solvent mixtures studied. Preferential solvation of

dx.doi.org/10.1021/jp310379h | J. Phys. Chem. B 2012, 116, 14433−14440

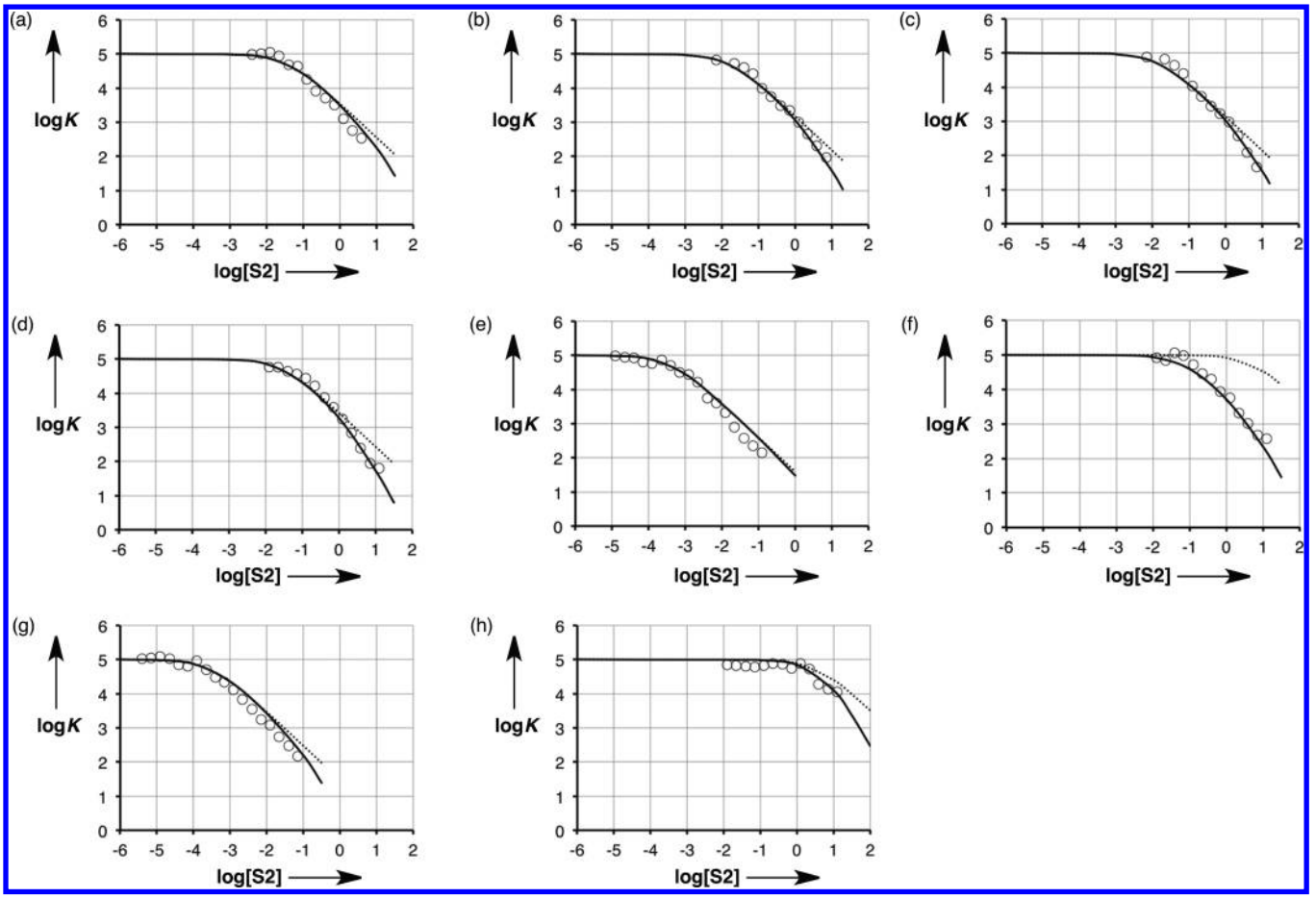

Figure 7. Association constant for formation of the D•A complex (K) plotted as a function of the concentration of S2 in mixtures of *n*-octane and a more polar solvent (S2). S2 is (a) di-*n*-octyl ether, (b) ethyl heptanoate, (c) 2-heptanone, (d) *n*-butyl cyanide, (e) *N*,*N*-diethyl acetamide, (f) 1,1,2,2-tetrachloroethane, (g) di-*n*-butyl sulfoxide, and (h) toluene. Dotted lines represent the log K profile calculated using eq 1, and solid lines represent the log K profile calculated using eq 4.

the solutes occurs at low S2 concentrations for highly polar solvents, such as sulfoxides, and requires much higher concentrations of S2 for less polar solvents, such as toluene. This study indicates that the solvation properties of solvent mixtures can be understood by considering the thermodynamic contributions of specific intermolecular contacts between the functional groups present in solution. A simple model (Figure 2) can be used to make predictions about the thermodynamic properties of solvent mixtures where the properties are dominated by one type of solvation interaction. Deviations from this model occur for solvents that are present in sufficiently high concentrations to preferentially solvate both H-bond donor and acceptor solutes. This is the case for solvents such as alcohols, acids, primary and secondary amides, and a more complex treatment of solvent self-association will be necessary for these systems.

■ EXPERIMENTAL SECTION

All solvents were HPLC grade and were used without further purification. A and D were purchased from Aldrich, and A was dried in a vacuum desiccator over phosphorus pentaoxide before use.

Automated UV−vis Titrations. Association constants were determined using a BMG Labtech Fluorostar Optima plate reader with a Hellma 96-well quartz microplate. Two host stock solutions were prepared from accurately weighed samples of D (5 mg) dissolved in S1 and in S2 in 25 mL volumetric flasks, to give a concentration of 1 mM in each. Five guest stock solutions were prepared by dissolving an accurately weighed sample of A (0.5 g) in S1 in a 5 mL volumetric flask to give a 0.46 M stock solution of A (stock solution 1). A serial dilution was carried out, whereby 570 μL of stock solution 1 was transferred to a 5 mL volumetric flask, which was then filled with S1 to give stock solution 2 (5.2×10^{-2} M). Stock solution 2 was diluted three more times in the same way to give stock solutions 3, 4, and 5, with concentrations of 5.9×10^{-3}, 6.6×10^{-4}, and 7.5×10^{-5} M. Similarly, five stock solutions of A were prepared in solvent S2.

These stock solutions were loaded onto a 96-well quartz microplate using purpose-written protocols with the plate reader. A total of 15 μL of the stock solution of D dissolved in S1 was pipetted into wells 1−48, and 15 μL of the stock solution of D dissolved in S2 was pipetted into wells 49−96. A gradient of concentrations of A was set up across the microplate to give a titration in S1 in wells 1−48 and a titration in S2 in wells 49−96. Incremental amounts of stock solutions 4 and 5 of A were pipetted into wells 31−48, then incremental amounts of stock solutions 2 and 3 were pipetted into wells 11−30, and incremental amounts of stock solution 1 were pipetted into wells 1−10. A similar procedure was used to add A to wells 49−96. The total volume in each well was made up to 150 mL by adding the relevant pure solvent.

dx.doi.org/10.1021/jp310379h | J. Phys. Chem. B 2012, 116, 14433−14440

The absorbance of each well was measured at 6 wavelengths (260, 280, 340, 390, 420, and 600 nm) to obtain UV/vis titration data sets in S1 and in S2. Ten μL aliquots of S1 were added to wells 1−48, 10 μL aliquots of S2 were added to wells 49−96, and the plate was agitated to ensure mixing. The UV/vis absorption of the plate was recorded giving two more titration data sets in two different solvent mixtures. This procedure was repeated until the wells were full (320 μL), to give binding isotherms over the entire volume fraction range from pure S1 to pure S2. The output was an excel spreadsheet, which was analyzed using the Solver routine to optimize a binding constant for each solvent composition (K), the extinction coefficient of the free host (ε_f), the extinction coefficient of the bound host (ε_b), and the extinction coefficient of the guest (ε_A) to give a calculated absorbance (A_{calc}) that matched the experimental absorbance (A_{expt}) at each of the six wavelengths (eqs 5 and 6). Dilution of the host and guest occurs during the solvent addition, and this was taken into account in the fitting.

$$A_{calc} = \varepsilon_A[A] + \varepsilon_f[D]_f + \varepsilon_b[D]_b \quad (5)$$

$$[D]_b = \left[1 + K[A]_0 + K[D]_0 - \sqrt{(1 + K[A]_0 + K[D]_0)^2 - 4K^2[A]_0[D]_0}\right]/2K \quad (6)$$

where $[D]_b$ is the concentration of bound host, $[D]_f$ is the concentration of free host, and $[D]_0$ and $[A]_0$ are the total concentrations of host and guest, respectively.

In order to access low concentrations of the more polar solvents in the solvent mixtures, the composition of "S2" used in the protocol above was varied by using mixtures of the polar solvent and *n*-octane. Thus "S2" in the protocol above could be either pure polar solvent or as dilute as a 0.001% by volume mixture with *n*-octane.

Manual UV−vis Titrations. Manual titrations were carried out using a Cary 3 Bio UV−vis spectrophotometer. A 4 mL sample of the host (D) was prepared at a known concentration of about 0.02 mM in *n*-octane. A total of 0.7 mL of this solution was removed and added to a 1 mL quartz cuvette and the UV−vis spectrum was recorded. The guest (S2) was then dissolved in the remaining host solution, aliquots of this solution were added successively to the cuvette, and the UV−vis absorption spectrum was recorded after each addition. Changes in UV−vis absorption were analyzed using Microsoft Excel, and the data fit well to a 1:1 binding isotherm allowing for a second weaker nonspecific binding event.

NMR Titrations. ^{31}P NMR titrations were carried out using a Bruker Avance III 400 spectrometer. A 4 mL sample of the host (A) was prepared at a known concentration of about 20 mM. A total of 0.5 mL of this solution was removed, and a ^{31}P NMR spectrum was recorded. A capillary containing 5 mM methylene diphosphonic acid in D_2O was used to provide a ^{31}P reference signal (17.98 ppm) and a deuterium lock signal. The guest (S2) was then dissolved in the remaining host solution, aliquots of this solution were added successively to the NMR tube, and the ^{31}P NMR spectrum was recorded after each addition. The observed changes in chemical shift were analyzed using Microsoft Excel. The data fit well to a 1:1 binding isotherm allowing for a second weaker nonspecific binding interaction.

■ ASSOCIATED CONTENT

Supporting Information

Representative titration data for the automated and manual UV/vis titration experiments. This material is available free of charge via the Internet at http://pubs.acs.org.

■ AUTHOR INFORMATION

Corresponding Author

*E-mail: c.hunter@sheffield.ac.uk.

Notes

The authors declare no competing financial interest.

■ ACKNOWLEDGMENTS

We thank the EPSRC and the James Black Foundation for funding.

■ REFERENCES

(1) Muanda, M. W.; Nagy, J. B.; Nagy, O. B. *Tetrahedron Lett.* **1974**, 3421−3424.
(2) Nagy, O. B.; Muanda, M. W.; Nagy, J. B. *J. Chem. Soc. Faraday Trans. 1* **1978**, *74*, 2210−2228.
(3) Covington, A. K.; Newman, K. E. *Adv. Chem. Serv.* **1976**.
(4) Covington, A. K.; Newman, K. E. *Pure Appl. Chem.* **1979**, *51*, 2041−2058.
(5) Lerf, C.; Suppan, P. *J. Chem. Soc. Faraday Trans.* **1992**, *88*, 963−969.
(6) Suppan, P. *J. Chem. Soc. Faraday Trans. 1* **1987**, *83*, 495−509.
(7) Silva, P. L.; Bastos, E. L.; El Seoud, O. A. *J. Phys. Chem. B* **2007**, *111*, 6173−6180.
(8) El Seoud, O. A. *Pure Appl. Chem.* **2007**, *79*, 1135−1151.
(9) Suganthi, G.; Sivakolunthu, S.; Ramakrishnan, V. *J. Fluores.* **2010**, *20*, 1181−1189.
(10) Umadevi, M.; Kumari, M. V.; Bharathi, M. S.; Vanelle, P.; Terme, T. *Spectrochim. Acta Part A* **2011**, *78*, 122−127.
(11) Petrov, N. K. *High Energy Chem.* **2006**, *40*, 22−34.
(12) Wetzler, D. E.; Chesta, C.; Fernandez-Prini, R.; Aramendia, P. F. *Pure Appl. Chem.* **2001**, *73*, 405−409.
(13) Frankel, L. S.; Langford, C. H. *J. Phys. Chem.* **1970**, *74*, 1376−1381.
(14) Remerie, K.; Engberts, J. *J. Phys. Chem.* **1983**, *87*, 5449−5455.
(15) Diaz, M. D.; Berger, S. *Magn. Reson. Chem.* **2001**, *39*, 369−373.
(16) Saielli, G.; Bagno, A. *Phys. Chem.* **2010**, *12*, 2981−2988.
(17) Seba, H. B.; Thureau, P.; Ancian, B.; Thevand, A. *Magn. Reson. Chem.* **2006**, *44*, 1109−1117.
(18) Thureau, P.; Ancian, B.; Viel, S.; Thevand, A. *Chem. Commun.* **2006**, 1884−1886.
(19) Symons, M. C. R. *Pure Appl. Chem.* **1986**, *58*, 1121−1132.
(20) Meade, M.; Hickey, K.; McCarthy, Y.; Waghorne, W. E.; Symons, M. C. R.; Rastogi, P. P. *J. Chem. Soc. Faraday Trans.* **1997**, *93*, 563−568.
(21) Bertie, J. E.; Lan, Z. D. *J. Phys. Chem. B* **1997**, *101*, 4111−4119.
(22) Takamuku, T.; Tanaka, M.; Sako, T.; Shimomura, T.; Fujii, K.; Kanzaki, R.; Takeuchi, M. *J. Phys. Chem. B* **2010**, *114*, 4252−4260.
(23) Devalera, E.; Feakins, D.; Waghorne, W. E. *J. Chem. Soc. Faraday Trans. I* **1983**, *79*, 1061−1071.
(24) Kamineska-Piotrowicz, E. *Thermochim. Acta* **2005**, *427*, 1−7.
(25) Bouteiller, L.; van der Schoot, P. *J. Am. Chem. Soc.* **2012**, *134*, 1363−1366.
(26) Khatri, C. A.; Pavlova, Y.; Green, M. M.; Morawetz, H. *J. Am. Chem. Soc.* **1997**, *129*, 6991−6995.
(27) Rastrelli, F.; Saielli, G.; Bagno, A.; Wakisaka, A. *J. Phys. Chem. B* **2004**, *108*, 3479−3487.
(28) Marcus, Y. *Solvent Mixtures Properties and Selective Solvation*; Marcel Dekker Inc.: New York, 2002.
(29) Montagna, M.; Sterpone, F.; Guidoni, L. *J. Phys. Chem. B* **2012**, *116*, 11695−11700.

(30) Cook, J. L.; Hunter, C. A.; Low, C. M. R.; Perez-Velasco, A.; Vinter, J. G. *Angew. Chem., Int. Ed.* **2008**, *47*, 6275−6277.
(31) Buurma, N. J.; Cook, J. L.; Hunter, C. A.; Low, C. M. R.; Vinter, J. G. *Chem. Sci.* **2010**, *1*, 242−246.
(32) Amenta, V.; Cook, J. L.; Hunter, C. A.; Low, C. M. R.; Vinter, J. G. *Org. Biomol. Chem.* **2011**, *9*, 7571−7578.
(33) Hunter, C. A. *Angew. Chem., Int. Ed.* **2004**, *43*, 5310−5324.
(34) Abraham, M. H.; Grellier, P. L.; Prior, D. V.; Duce, P. P.; Morris, J. J.; Taylor, P. J. *J. Chem. Soc. Perkin Trans. 2* **1989**, 699−711.
(35) Cabot, R.; Hunter, C. A. *Org. Biomol. Chem.* **2010**, *8*, 1943−1950.
(36) Cabot, R.; Hunter, C. A.; Varley, L. M. *Org. Biomol. Chem.* **2010**, *8*, 1455−1462.